Basic mechanism for abrupt monsoon transitions

Anders Levermann[a,b,1], Jacob Schewe[a,b], Vladimir Petoukhov[a], and Hermann Held[a]

[a]Earth System Analysis, Potsdam Institute for Climate Impact Research, 14473 Potsdam, Germany; and [b]Institute of Physics, Potsdam University, 14473 Potsdam, Germany

Monsoon systems influence the livelihood of hundreds of millions of people. During the Holocene and last glacial period, rainfall in India and China has undergone strong and abrupt changes. Though details of monsoon circulations are complicated, observations reveal a defining moisture-advection feedback that dominates the seasonal heat balance and might act as an internal amplifier, leading to abrupt changes in response to relatively weak external perturbations. Here we present a minimal conceptual model capturing this positive feedback. The basic equations, motivated by observed relations, yield a threshold behavior, robust with respect to addition of other physical processes. Below this threshold in net radiative influx, R_c, no conventional monsoon can develop; above R_c, two stable regimes exist. We identify a nondimensional parameter l that defines the threshold and makes monsoon systems comparable with respect to the character of their abrupt transition. This dynamic similitude may be helpful in understanding past and future variations in monsoon circulation. Within the restrictions of the model, we compute R_c for current monsoon systems in India, China, the Bay of Bengal, West Africa, North America, and Australia, where moisture advection is the main driver of the circulation.

Earth system | tipping element | abrupt climate change | atmospheric circulation | nonlinear dynamics

Monsoon rainfall shapes regional culture and the livelihoods of hundreds of millions of people (e.g., 1, 2). The future evolution of monsoon rainfall under increasing levels of atmospheric CO_2 and aerosol pollution is highly uncertain (3). Although greenhouse gas abundance tends to increase monsoon rainfall strength (4–6), the situation is more complex with changing aerosol distribution (7, 8). Given this large uncertainty in the future forcing of monsoons, it is crucial to understand internal monsoon dynamics, especially with respect to self-amplifying feedbacks, which might result in potentially strong responses to small perturbations. Zickfeld et al. (2005) found two stable states in a simple model of the Indian summer monsoon, which in principle allows for rapid transition between radically different monsoon circulations (9, 10) and thereby identified the Indian monsoon as a potential tipping element of the climate system (11). Evidence for such behavior is found in paleodata that show rapid and strong variations in Indian and East Asian monsoon rainfall (12, 13). These abrupt changes have been linked to climatic events in the North Atlantic for the last glacial period (14, 15) as well as for the Holocene (16, 17). Though a physical mechanism for this teleconnection has been suggested (18), relevant climatic signals of the North Atlantic events in Asia (such as temperature and moisture anomalies) are very small (19) indicating that internal feedbacks in monsoon dynamics may have amplified the weak external forcing.

Both spatial patterns and temporal evolution of monsoon rainfall are influenced by a number of physical processes (7, 18, 20–28) as well as characteristics of vegetation (29–31) and topography (32). Though these details are crucial for the specific behavior of different monsoon systems and their significance will vary from region to region, there exist defining processes fundamental to any monsoon dynamics (e.g. 33, 34). These processes are the advection of heat and moisture during monsoon season and the associated rainfall and release of latent heat. In accordance with Zickfeld

et al. (9), we suggest the positive moisture-advection feedback (21) as a candidate for the main cause of abrupt changes in monsoon dynamics.

We derive a minimal conceptual model of a monsoon circulation (Fig. 1*A*), comprising merely conservation of heat and moisture, knowingly neglecting a large number of relevant physical processes in order to distill the fundamental nonlinearity of monsoon circulations. The resulting governing equation exhibits the necessary solution structure to explain qualitatively both strong, persistent changes in monsoon rainfall, as observed in paleorecords, and abrupt variablity within one rainy season. This equation's dynamic similitude, expressed through a single dimensionless number l, which defines the threshold behavior and makes different monsoon systems comparable with respect to their transition, may serve as a building block for understanding past and future abrupt changes in monsoon dynamics.

Results

Moisture-Advection Feedback in Monsoon Dynamics. The seasonal evolution of the continental heat budget for different monsoon systems (Fig. 2) shows that sensible heat flux from the land surface increases during spring and heats up the atmospheric column prior to the rainy season. The onset of heavy rainfall (red vertical lines in Fig. 2) is associated with a drop in surface temperature on land, and consequently, sensible heat flux reduces drastically. During the monsoon season, latent heat release dominates the atmospheric heat content, whereas net radiative fluxes are relatively constant throughout the year, reflecting the stabilizing long-wave radiative feedback. In response to the latent heat release, thermal energy is transported out of the region through large-scale advection and synoptic processes. The main dynamical driver of the monsoon is therefore the positive moisture-advection feedback (Fig. 1*A*): The release of latent heat from precipitation over land adds to the temperature difference between land and ocean, thus driving stronger winds from ocean to land and increasing in this way landward advection of moisture, which leads to enhanced precipitation and associated release of latent heat. In the following, we seek to capture this feedback in a minimal conceptual model.

Minimal Conceptual Model for Abrupt Monsoon Transitions. For this purpose, consider the heat-balance equation of the monsoon season (Fig. 2, for example at blue vertical line).

$$\mathcal{L} \cdot P - \epsilon C_p W \cdot \Delta T + R = 0, \qquad [1]$$

where latent heat release and net radiation into the atmospheric column, R, balance heat divergence, and the relatively weak contribution from sensible heat transport from the land surface to the atmospheric column has been neglected. ΔT is the atmospheric
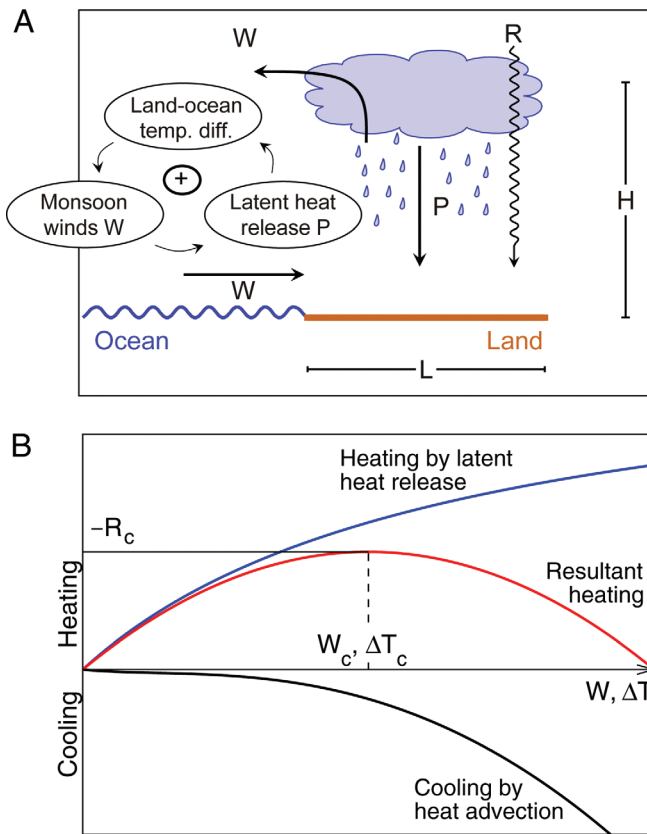
Fig. 1. Basic mechanism of abrupt monsoon transitions. (*A*) Geometry of conceptual model and fundamental moisture-advection feedback. The same notation as in the text is used for wind *W*, precipitation *P*, net radiative influx *R*, vertical scale *H* and horizontal scale *L*. Arrows in the feedback loop indicate the amplification of one physical processes by another. (*B*) Mechanism of the abrupt transition. Heating by latent heat release and cooling through heat advection compensate each other, and both decrease with decreasing winds (or equivalently, land–ocean temperature difference ΔT; see Eq. **2**). The resultant heating balances the negative net radiative flux as long as it is above a threshold R_C, below which no conventional monsoon exists.

temperature difference between land and ocean. Latent heat of condensation is $\mathcal{L} = 2.6 \cdot 10^6 J/kg$ and volumetric heat capacity of air at constant pressure $C_p = 1,295 \ J/m^3/K$. *P* is the mean precipitation over land (in $kg/m^2/s$). The ratio $\epsilon = H/L$ between vertical extent *H* of the lower troposphere and the horizontal scale *L* of the region of precipitation (Fig. 1) enters because of the balance of the horizontal advective heat transport and the vertical fluxes of net radiative influx *R* and precipitation *P*. A length scale for the coastline drops out. Note that no annual cycle is included in the model. Only budgets for the rainy season are considered. Consequently, this model does not capture any interseasonal or any interannual dynamics. Equations are only valid for landward winds, $W \geq 0$.

Assuming dominance of ageostrophic flow in low latitudes, the landward mean wind *W* is taken to be proportional to the temperature difference between land and ocean (33, 36, 37):

$$W = \alpha \cdot \Delta T. \qquad [2]$$

This assumption of a linear relation between the two quantities is supported by National Centers for Environmental Prediction/National Center for Atmospheric Research (NCEP/NCAR) reanalysis data (Fig. 3) with correlation coefficients above 50% for all regions. There is significant scatter in some plots, reflecting the fact that other processes may be relevant for the monsoon dynamics in the corresponding regions. A possible offset, as observed in

some regions, does not alter the model behavior qualitatively. This offset is discussed together with other possibly relevant processes in the *SI Appendix*. Here we seek to capture only processes relevant to the self-amplification feedback. Neglecting the effect of evaporation over land and associated soil-moisture processes in the continental moisture budget, precipitation has to be balanced by the net landward flow of moisture

$$\epsilon W \cdot \rho(q_O - q_L) - P = 0, \qquad [3]$$

where q_O and q_L are specific humidity over ocean and land, and $\rho = 1.3 \ kg/m^3$ is mean air density.

Note that evaporation is clearly an important process for the moisture budget (e.g. (38)) and is omitted in Eq. **3** only for the sake of clarity. Including evaporation does not change the model behavior qualitatively (see *SI Appendix*). It does, however, shift the value of the critical threshold, as we will show in the next section when applying our model to data. In the minimalistic spirit of this section, we omit the effect of evaporation here because it is not of first order to the problem. Consistent with reanalysis data (Fig. 4) and theoretical considerations (36, 39), continental rainfall is assumed to be proportional to the mean specific humidity within the atmospheric column

$$P = \beta q_L. \qquad [4]$$

The effect of an offset between these quantities does not change the model behavior qualitatively (see *SI Appendix*). This set of assumptions (Eqs. **1–4**) yields the dimensional governing equation of the model

$$W^3 + \frac{\beta}{\epsilon\rho}W^2 - \frac{\alpha}{\epsilon C_p}(\mathcal{L}q_O\beta + R) \cdot W - \frac{\alpha\beta}{\epsilon^2\rho C_p} \cdot R = 0. \qquad [5]$$

Note that through the linear relation of Eq. **2**, this equation can equally be understood as an expression for the temperature difference beween land and ocean ΔT, which might be more useful for some applications. Introduction of nondimensional variables $w \equiv W\epsilon\rho/\beta$ and $p = P/(q_O\beta)$ results in the nondimensional equation

$$w^3 + w^2 - (l + r)w - r = 0, \qquad [6]$$

which depends on two parameters only: The dimensionless net radiative influx $r \equiv R \cdot \epsilon\alpha\rho^2/(C_p\beta^2)$ and a measure for the relative role of latent and advective heat transport

$$l \equiv (\epsilon\alpha\rho^2 \mathcal{L}q_O)/(C_p\beta) = (\mathcal{L}q_O\beta)/(C_p\beta^2/(\epsilon\alpha\rho^2)). \qquad [7]$$

Large *l* corresponds to a strong influence of moisture advection (scaling as $\mathcal{L}q_O\beta p$) on the continental heat budget compared with heat advection by large-scale and synoptic processes (scaling as $C_p\beta^2 w^2/(\alpha\epsilon\rho^2)$). The nondimensional precipitation is directly related to the wind through $p = w/(1 + w)$.

Solutions $w(r)$ of Eq. **6** are determined entirely by a choice of the only free parameter *l*, which can be expressed in terms of a critical threshold of net radiative flux r_c, below which no physical solution exists (Fig. 5). The critical point (r_c, w_c) will vary for different monsoon systems. It is directly linked to the only remaining parameter *l*, through

$$w_c(w_c + 1)^2 = l/2. \qquad [8]$$

and therefore uniquely defines the solution $w(r)$ of the model. The critical radiation can be computed from

$$r_c = -w_c^2(2w_c + 1) \qquad [9]$$

Thus for large *l* (as observed in some monsoon systems) the critical threshold is well approximated by $r_c \approx -l$. Note that *l* is scaling like $q_O\alpha/\beta$ where α and β have clear-cut physical meaning (39). α is essentially a function of the near-surface cross-isobar angle and thereby a function of surface roughness and static stability of the
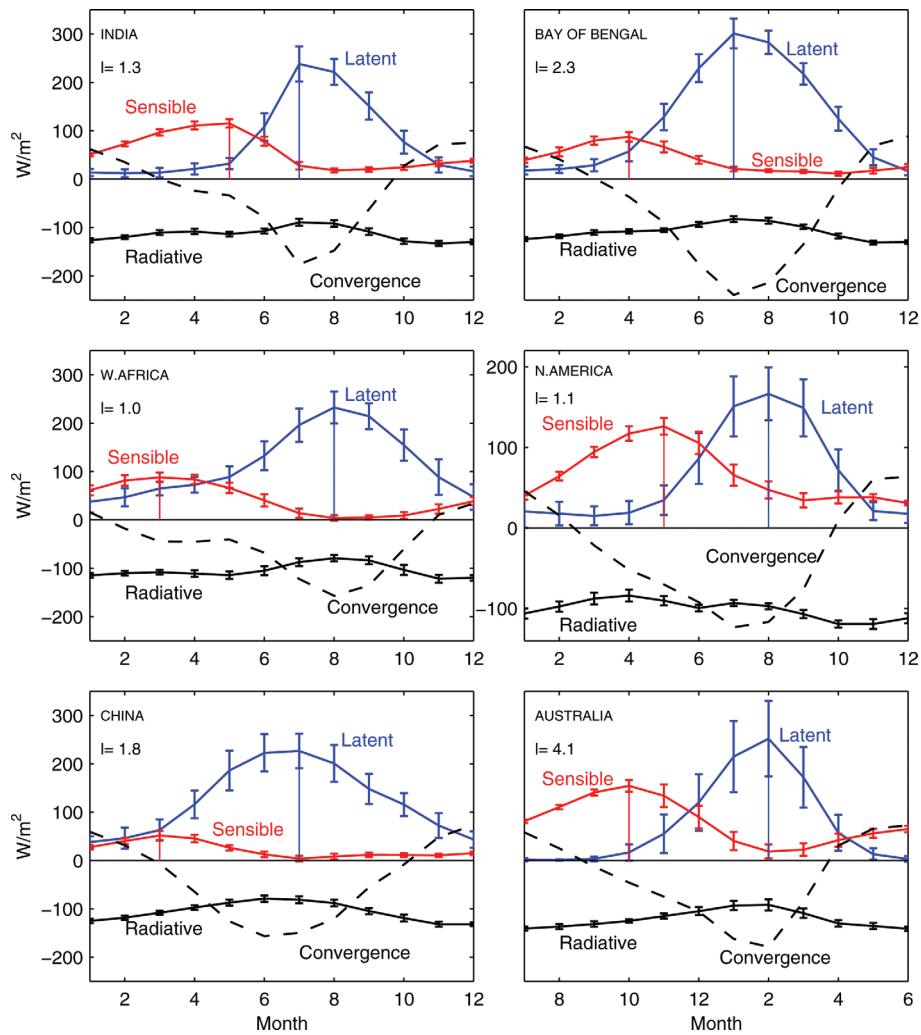
Fig. 2. Seasonal heat contributions to the atmospheric column over different continental monsoon regions in NCEP/NCAR reanalysis data (35). Radiative heating of the land surface in spring enhances sensible heat flux from the ground ('Sensible'). During the rainy season, latent heat release dominates the heat budget ('Latent'). Radiative heat flux comprises all radiative fluxes in and out of the atmospheric column ('Radiative'). The excess heat is transported out of the continental monsoon region though large-scale advective and synoptic processes ('Convergence'). Error bars give the standard deviation from the 60 years for which data is available (1948–2007). Regions from which values were taken are defined in the (*SI Appendix*). The red and blue vertical lines emphasize the months of maximum sensible heat flux and latent heat flux, respectively.

planetary boundary layer (PBL). β is governed by the characteristic turnover (recycling) time of liquid water in the atmosphere and thereby determined by static stability and vertical velocity in the PBL. Any physical solution for $r > r_c$ is characterized by landward winds $w > 0$ and positive precipitation $p > 0$.

Let us now try to understand the physical mechanism behind the threshold behavior observed in Fig. 5. In the tropics net radiative influx is negative, i.e. radiation cools the atmospheric column. During monsoon season the same is true for the advection of heat by the winds because winds blow predominantly from the colder oceanic surrounding. The release of latent heat compensates for both of these heat-loss processes. If monsoon winds get weaker, condensation and therefore latent heat release through precipitation are reduced (moisture-advection feedback, Fig. 1*A*). The abruptness of the transition emerges through an additional stabilizing effect of the direct heat advection which is cooling the atmospheric column and is also reduced for reduced monsoon winds. Thus both advection-related processes, precipitative warming and thermal cooling, are simultaneously reduced and partly compensate until a threshold is reached at which condensation/precipitation cannot provide the necessary latent heat to sustain a circulation. As a consequence, land-ocean

temperature difference ΔT and therewith monsoon winds break down (Fig. 1*B*).

Estimate of Critical Threshold for Current Monsoon Systems. In order to estimate the critical threshold of different monsoon systems within the limitation of this very simple model, we use time series of precipitation P, radiation R, temperature difference ΔT, and specific humidity q_O from the NCEP/NCAR reanalysis data (35) to compute time series for $\alpha(t) = (\mathcal{L}P + R)/(\epsilon C_p \Delta T^2)$ and $\beta(t) = ((\mathcal{L}P+R) \cdot \rho P)/((\mathcal{L}P+R)q_O\rho - C_p\Delta TP)$, assuming applicability of the model and stationary statistics within the observational period (1948-2007). Via $\alpha(t)$ and $\beta(t)$, the parameter $l(t)$ is known and the system is estimated for each year. As a simple test for the model, we calculate the remaining quantity that is not used for the computation of $\alpha(t)$ and $\beta(t)$, the specific humidity over land

$$ q_L'(t) = q_O(t) - \frac{C_P \Delta T(t) P(t)}{\rho(\mathcal{L}P(t) + R(t))}. \qquad [10] $$

The resulting model estimate of the specific humidity q_L' compares reasonably well (Fig. S2 in the *SI Appendix*) with the independently observed q_L that was used in Fig. 4 to motivate the relation between specific humidity and precipitation (Eq. **4**).
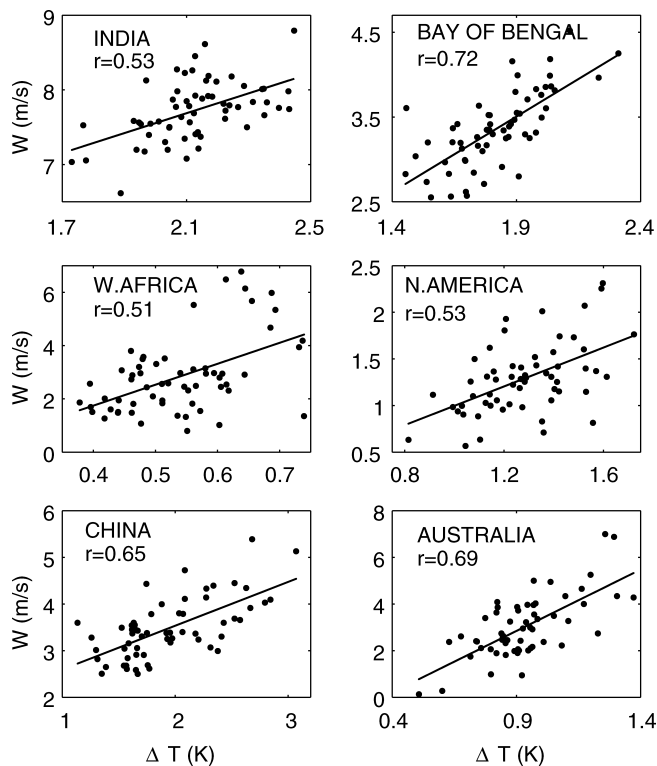
Fig. 3. Landward zonal wind versus temperature difference between land and ocean during monsoon season [NCEP/NCAR reanalysis data (35)]. The lines show best linear regression with correlation r.

Via the definition of l, we compute R_c from the time series $\alpha(t)$ and $\beta(t)$ for each year between 1948-2007. Note that the only quantity that is not constrained by data in this computation is the parameter ϵ, which defines the ratio of vertical and horizontal scale. However, the critical threshold R_C is independent of ϵ, and thus the calculation depends only on relatively robust averaged values of precipitation, net radiation, average temperature difference between land and ocean, specific humidity over ocean, and the natural constants ρ, $\mathcal{L}$, and C_p. We interpret the resulting distribution of the critical threshold R_c (Fig. 6, blue) as a noisy estimate of a stationary critical threshold.

Within the limitations of the model, the observed net radiation is higher than the critical threshold in the Bay of Bengal, West Africa, and China. In India, North America, and Australia, the distributions have significant overlap. Incorporating evaporation into the model shifts the distribution toward lower thresholds (Fig. 6, red), while at the same time increasing the precipitation threshold P_c. Standard bootstrapping (see *SI Appendix*) reveals that the estimates in Fig. 6 are already relative robust distributions, in view of the simplicity of the model approach.
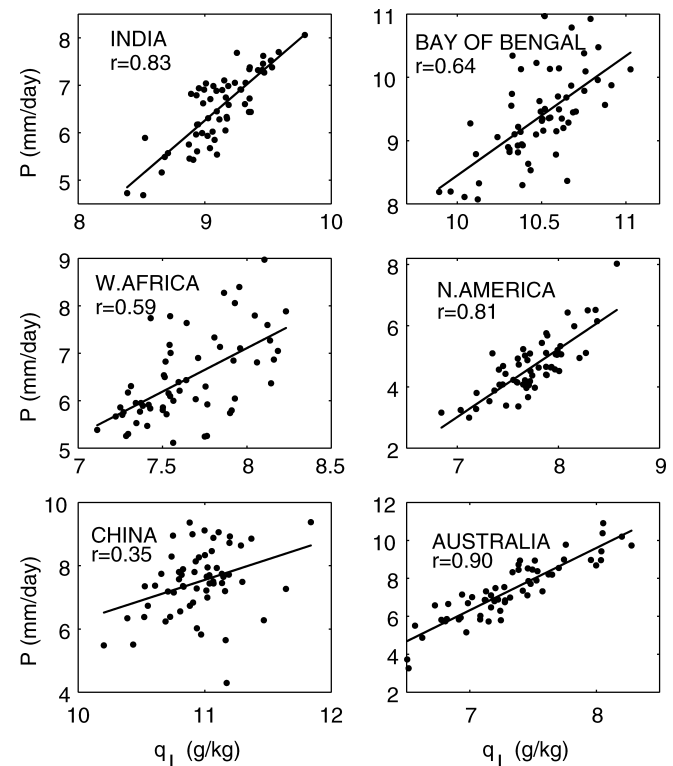
Discussion

A minimal conceptual model for monsoon circulations that captures the moisture-advection feedback is presented. The model is unlikely to describe details of monsoon circulations quantitatively, nor is it meant to capture all dynamical processes of a monsoon circulation. Following a minimalistic philosophy, the model comprises the necessary processes for a positive feedback and thereby demonstrates the possibility of an abrupt transition of monsoon circulations from a state with strong rainfall to a weak precipitation state. All model equations are backed by relations found in NCEP/NCAR reanalysis data. For India, it has been shown that this data-set properly represents the statistics of precipitation when compared with regional observations with higher spatial resolution (40).

Because the processes represented in our model are fundamental to monsoon systems, we believe that the results strongly suggest the possibility of abrupt monsoon transitions. Because the dominant driving process is captured, it is not impossible that the model can provide a reasonable estimate for the critical threshold, R_c, once all necessary processes are incorporated. The bifurcation structure of the model is robust with respect to incorporation of other physical processes (see *SI Appendix*) and only changes qualitatively when either of these perturbations dominate the dynamics. Thus, the applicability of our model is based on the assumption that moisture advection is the dominant process in the heat budget of a monsoon system.

The possibility of abrupt transition is due to the competition of the main heat transport processes during the rainy season. Although latent heat release through precipitation warms the atmospheric column, direct advection of heat is cooling it. Both processes decrease with decreasing monsoon winds and thereby compensate each other with respect to the net heat injection into the atmospheric column. The threshold of this stabilizing effect is set by the radiative cooling, which is characteristic to low-latitudes and is strongly influenced by aerosol distribution in the region.

According to our model, abrupt transitions may occur in two different ways. For net radiation above the critical threshold $R > R_C$, the system is bistable. Because the model only describes the rainy season and does not capture the annual monsoon cycle, abrupt transitions in the bistable regime can only be interpreted intraseasonally, e.g., a month of heavy rain followed by a month of extraordinarily weak precipitation. An example could be the extremely weak rainfall in July and September observed in India in the year 2002, in which the rest of the season exhibited average rainfall (41).

Our model does not capture the dynamics of a decline or increase in monsoon strength over several years. Thus, paleodata in which strong variation in monsoon rainfall have been recorded cannot be explained by the bistable regime because these recordings show monsoon changes over several years, decades, or

Fig. 4. Precipitation versus specific humidity over land during monsoon season [NCEP/NCAR reanalysis data (35)]. The lines show best linear regression with correlation r.

Fig. 5. Solution of the nondimensional governing Eq. **6**. (*Top*) Nondimensional landward wind for two values of the only parameter $l = 0$ and $l = 1$. (*Middle*) Corresponding nondimensional precipitation. (*Bottom*) Nondimensional precipitation for higher values of l as observed in some monsoon systems. The functional form of the solution is not changed qualitatively. The critical threshold $(w_c(l), p_c(l))$ is given as the black curve in each frame.

Fig. 6. State of current monsoon systems with respect to the critical point computed from the conceptual model. The black distribution reflects observed fluctuations in net radiation in the different monsoon systems. The blue distribution provides the computed critical threshold from the conceptual model. The red distribution includes the effect of evaporation. Lines give a Gaussian function with the same mean and standard deviation as the corresponding discrete distribution.

even centuries. Such behavior would correspond to a shift of the system across the critical threshold into the monostable regime $R < R_C$ without a conventional monsoon. If persistent, such a shift would be visible in paleorecords.

The reduction of the full set of model parameters to a single scaling number l, which determines the system and thereby the critical threshold, testifies to a remarkable dynamic similitude with respect to the atmospheric quantities α, β, and q_0. Different monsoon systems with the same l will have the same transition behavior. As illustrated in Fig. 5, l provides a measure for the position and the sharpness of the transition, i.e., for the point (r_c, w_c) in state space. This means, in particular, that a decrease in inflowing humidity q_0 associated with, e.g., colder climate conditions (which would decrease the threshold R_c and shift the system closer to a collapse) could be compensated by decreasing β, representing a lower turnover (recycling) time of moisture in the atmosphere, which is influenced by, e.g., aerosols.

The parameter q_0 in our model can be interpreted in a rather broad sense as a specific humidity of the vicinity influencing a monsoon region. As an example, the years with anomalously high snow cover over the Tibetan Plateau in spring and early summer (20, 26) could be characterized by a decrease in q_0 during midsummer, which would shift the threshold value R_c for the Indian monsoon closer to the observed precipitation over the region, thus increasing a possibility of monsoon breakdown in those years. Similarly, a colder climate with generally decreased humidity q_O could be closer to the critical threshold, which might be the reason for less-stable monsoon circulations during glacial periods.

In the future, net radiation may be reduced through aerosol pollution, which will push the system qualitatively closer to the critical threshold (7). On the Indian subcontinent, in China, and in parts of sub-Saharan Africa, agricultural productivity is closely linked to and limited by monsoon rainfall. Food security in these regions is particularly sensitive to monsoon variability (42–45). Studies with comprehensive models are necessary to confirm or reject the idea of the existence of a threshold as well as its position.

1. Auffhammer M, Ramanathan V, Vincent JR (2006) Integrated model shows that atmospheric brown clouds and greenhouse gases have reduced rice harvests in India. *Proc Natl Acad Sci USA* 103:19668–19672.
2. Zhang P, et al. (2008) A test of climate, sun, and culture relationships from an 1810-year chinese cave record. *Science* 322:940–942.
3. Patra PK, Behera SK, Herman JR, Akimoto S, Yamagata T (2005) The indian summer monsoon rainfall: Interplay of coupled dynamics, radiation and cloud microphysics. *Atmos Chem Phys Discuss* 5:2879–2895.
4. Meehl GA, Washington WM (1993) South Asian summer monsoon variability in a model with doubled atmospheric carbon dioxide concentration. *Science* 260:1101–1104.
5. Zwiers FW, Kharin VV (1998) Changes in the extremes of the climate simulated by CCC GCM2 under CO2 doubling. *J Climate* 11:2200–2222.
6. May W (2002) Simulated changes of the Indian summer monsoon under enhanced greenhouse gas conditions in a global time-slice experiment. *Geophys Res Lett* 29:1118.
7. Ramanathan V, et al. (2005) Atmospheric brown clouds: Impacts on South Asian climate and hydrological cycle. *Proc Natl Acad Sci USA* 102:5326–5333.
8. Lau KM, Kim KM (2006) Observational relationships between aerosol and asian monsoon rainfall, and circulation. *Geophys Res Lett* 33:L21810.
9. Zickfeld K, Knopf B, Petoukhov V, Schellnhuber HJ (2005) Is the indian summer monsoon stable against global change? *Geophys Res Lett* 32:L15707.
10. Knopf B, Zickfeld K, Flechsig M, Petoukhov V (2008) Sensitivity of the Indian monsoon to human activities. *Adv Atmos Sci* 25:932–945.
11. Lenton TM, et al. (2008) Tipping elements in the earth's climate system. *Proc Natl Acad Sci USA* 105:1786–1793.
12. Wang P, et al. (2005) Evolution and variability of the Asian monsoon system: State of the art and outstanding issues. *Quaternary Sci Rev* 24:595–629.
13. Wang Y, et al. (2008) Millennial- and orbital-scale changes in the East Asian monsoon over the past 224,000 years. *Nature* 451:1090–1093.
14. Overpeck JT, Anderson D, Trumbore S, Prell W (1996) The southwest Indian monsoon over the last 18000 years. *Climate Dynamics* 12:213–225.
15. Burns SJ, Fleitmann D, Matter A, Kramers J, Al-Subbary AA (2003) Indian ocean climate and an absolute chronology over Dansgaard/Oeschger events 9 to 13. *Science* 301:1365–1367.

16. Gupta AK, Anderson DM, Overpeck JT (2003) Abrupt changes in the Asian southwest monsoon during the Holocene and their links to the North Atlantic ocean. *Nature* 421:354–357.
17. Wang Y, et al. (2005) The Holocene Asian Monsoon: Links to solar changes and North Atlantic climate. *Science* 308:854–857.
18. Goswami BN, Madhusoodanan MS, Neema CP, Sengupta D (2006) A physical mechanism for North Atlantic SST influence on the Indian summer monsoon. *Geophys Res Lett* 33:L02706.
19. Zhang R, Delworth TL (2005) Simulated tropical response to a substantial weakening of the Atlantic Thermohaline Circulation. *J Climate* 18:1853–1860.
20. Hahn DG, Shukla J (1976) An apparent relationship between Eurasian snow cover and Indian monsoon rainfall. *J Atmos Sci* 33:2461–2462.
21. Webster PJ, et al. (1998) Monsoons: Processes, predictability, and the prospects for prediction. *J Geophys Res* 103:14451–14510.
22. Krishnamurthy V, Goswami BN (2000) Indian monsoon-ENSO relationship on inter-decadal timescale. *J Climate* 13:579–595.
23. Clark CO, Cole JE, Webster PJ (2000) Indian ocean SST and Indian summer rainfall: Predictive relationships and their decadal variability. *J Climate* 13:2503–2519.
24. Kucharski F, Molteni F, Yoo JH (2006) SST forcing of decadal Indian monsoon rainfall variability. *Geophys Res Lett* 33:L03709.
25. Goswami BN, Xavier PK (2005) ENSO control on the south Asian monsoon through the length of the rainy season. *Geophys Res Lett* 32:L18717.
26. Dash SK, Singh GP, Shekhar MS, Vernekar AD (2005) Response of the Indian summer monsoon circulation and rainfall to seasonal snow depth anomaly over Eurasia. *Climate Dynamics* 24:1–10.
27. Wang B (2005) *The Asian Monsoon* (Springer, Berlin).
28. Yang J, Liu Q, Xie SP, Liu Z, Wu L (2007) Impact of the Indian ocean SST basin mode of the Asian summer monsoon. *Geophys Res Lett* 34:L02708.
29. Meehl GA (1994) Influence of the land surface in the Asian summer monsoon: External conditions versus internal feedbacks. *J Climate* 7:1033–1049.
30. Claussen M (1997) Modeling bio-geophysical feedback in the African and Indian monsoon region. *Climate Dynamics* 54:247–257.
31. Robock A, Mu M, Vinnikov K, Robinson D (2003) Land surface conditions over Eurasia and Indian summer monsoon rainfall. *J Geophys Res* 108:4131.
32. Liu X, Yin Z (2002) Sensitivity of East Asian monsoon climate to the uplift of the Tibetan Plateau. *Palaeogeogr Palaeoclimatol Palaeoecol* 183:223–245.
33. Webster PJ (1987) The elementary monsoon. In *Monsoons*, eds Fein JS, Stephens PL (Wiley, New York), pp. 3-32.
34. Webster PJ (1987) The variable and interactive monsoon. In *Monsoons*, eds Fein JS, Stephens PL (Wiley, New York), pp. 269–330.
35. Kistler R, et al. (2001) The NCEP/NCAR 50-year reanalysis. *Bull Amer Meteor Soc* 82:247–267.
36. Petoukhov VK (1982) Two mechanisms of temperature oscillations in a thermo-dynamical model of the troposphere-stratosphere system. *Atmos Ocean Phys* 18: 126–137.
37. Brovkin V, Claussen M, Petoukhov V, Ganopolski A (1998) On the stability of the atmosphere- vegetation system in the Sahara/Sahel region. *J Geophys Res* 103:31613–31624.
38. Eltahir EAB (1998) A soil moisture-rainfall feedback mechanism: 1. theory and observations. *Water Resour Research* 34:765–776.
39. Petoukhov V, et al. (2000) CLIMBER-2: A climate system model of intermediate complexity. Part I: model description and performance for present climate. *Climate Dynamics* 16:1.
40. Goswami BN, Ramesh KV (2006) A comparison of interpolated NCEP (I-NCEP) rainfall with high-resolution satellite observations. *Geophysl Res Lett* 33:L19821.
41. Fasullo J (2005) Atmospheric hydrology of the anomalous 2002 Indian summer monsoon. *Monthly Weather Rev* 133:2996–3014.
42. Kumar KK, Kumar KR, Ashrit RG, Deshpande NR, Hansen JW (2004) Climate impacts in Indian agriculture. *Int J Climatol* 24:1375–1393.
43. Gregory PJ, Ingram JSI, Brklacich M (2005) Climate change and food security. *Philos Trans R Soc London Ser B* 360:2139–2148.
44. Haile M (2005) Weather patterns, food security and humanitarian response in sub-Saharan Africa. *Philos Trans R Soc London Ser B* 360:2169–2182.
45. Tao F, et al. (2004) Variability in climatology and agricultural production in China in association with the East Asian summer monsoon and El Niño Southern Oscillation. *Climate Res* 28:23–30.
46. Hansen J, et al. (1983) Efficient three-dimensional global models for climate studies: Models I and II. *Monthly Weather Rev* 111:609–662.

Basic mechanism for abrupt monsoon transitions

Anders Levermann * †, **Jacob Schewe** * † , **Vladimir Petoukhov** * , **and Hermann Held** *

*Earth System Analysis, Potsdam Institute for Climate Impact Research, Potsdam, Germany, and †Institute of Physics, Potsdam University, Potsdam, Germany

Supporting Information

Monsoon regions and definitions

NCEP/NCAR reanalysis data was obtained from http://www.cdc.noaa.gov/ as 60-year monthly mean time series, starting January 1948. Heat flux and precipitation data are averaged over land in each monsoon region. ΔT is the difference between the average temperatures over land and ocean. Humidities q_L and q_O refer to the same land and ocean regions, respectively. The near-surface, landward zonal wind velocity W is averaged over a third region. All three regions are given in table 1 and illustrated in figures S1 and S2, together with the respective definitions of the monsoon season that are used for the temporal averages shown in figures 3 and 4. W is averaged vertically between 850hPa and 1000hPa. q_O is averaged vertically between 600hPa and 1000hPa. All other vertical averages are over the entire atmospheric column.

Robustness of R_C estimate

In order to determine the statistical stability of the estimate of the distribution of R_C, we proceeded in two steps. (1) From the time series' autocorrelation we decided to treat the time series of α and β as containing virtually no memory, i.e. values from different years can be treated as statistically independent. Note that this assumption does not contradict the existence of interannual to decadal variability that is forced externally. (2) Via bootstrapping we generated surrogate time series of length 60. From this time series ensemble we found that the standard deviation of mean and standard deviation of the R_C-distribution are one order of magnitude below the standard deviation of the shown distribution of R_C-estimates. Hence the red curves in figure 6 are already relatively robust estimates, in view of the simplicity of the model approach.

Structural sensitivity of conceptual model

In order to analyse the structural robustness of the governing equation [6] to inclusion of further physical processes we start from the non-dimensional forms of the unperturbed equations [1] and [3]

$$lp - w^2 + r = 0 \qquad \text{[S1]}$$
$$w(1 - p) - p = 0 \qquad \text{[S2]}$$

using the same definitions of parameters l and r and non-dimensional variables w and p as in the main text. Note that the parameter l as computed from observations is of the order 10^4. Its qualitative influence on the solution structure can, however, already been seen for $l = 1$. Since 1 is the only other scale in the non-dimensional governing equation, we will use $l = 1$ as an example. Similarly we will show the qualitative influence of other paramters by setting them to 0.5 without claiming this to be an observed value. Note that for some cases the critical precipitation reduces and could in principle become zero or negative. This would change the model behaviour qualitatively. However this can only be the case when the corresponding process dominates the dynamics and is not merely a perturbation to the dynamics described in the core model. Non of the processes included eliminates the bifurcation for small parameter values. In this sense the model behaviour is robust.

Addition of evaporation. To our understanding, the strongest missing process is the effect of evaporation over land. In order to estimate the critical threshold of different monsoon systems we generalize the model by adding evaporation to the moisture budget (equation [3]). In the reanalysis data evaporation provides a very weak feedback within the dynamics and is well approximated by $P - E \approx \gamma P - E_O$, with region-specific constants E_0 and γ which is close to unity (figure S4). For this purpose we replace equation [S2] by $w(1 - p) - (\gamma p - e)$ with $e \equiv E_0/(\beta q_O)$. This equation can also be derived from the approach by Hansen et al. [1] and an additional assumption of constant total soil moisture within a rainy season. We obtain

$$p = \frac{w + e}{w + \gamma} \qquad \text{[S3]}$$

Accordingly, the governing equation transforms to

$$w^3 + \gamma w^2 - (l + r)w - (el + \gamma r) = 0 \qquad \text{[S4]}$$

Both constant and precipitaton-dependent evaporation shift critical radiation to lower and critical precipitation towards higher values (figure S5). As in the minimal model set-up, the critical threshold can be computed analytically from

$$w_c(w_c + \gamma)^2 = (\gamma - e)l/2 \qquad \text{[S5]}$$
$$r_c = 3w_c^2 + 2\gamma w_c - l$$

By additional use of the evaporation time series $E(t)$ from NCEP/NCAR reanalysis, the parameter e can be computed.

$$e = E(t)/(\beta q_O(t)) \qquad \text{[S6]}$$

By assuming γ to be constant (taken from the regression in figure S4), the critical threshold of this generalized model can be computed (figure 6).

Addition of cloud-albedo feedback. Assuming that cloud-albedo over land increases with the atmospheric moisture content we add a term $-a'q_L$ to equation [1] where a' is a constant. Consequently the nondimensional heat equation is transformed into

$$(l - a)p - w^2 + r = 0 \qquad \text{[S7]}$$

where $a \equiv a'q_O\epsilon\alpha/(C_p\beta^2)$. The governing equation

$$w^3 + w^2 - (l + r - a)w - r = 0 \qquad \text{[S8]}$$

shows the same functional form with an effective shift of the original l-parameter towards lower values (figure S6). This reduces the significance of the moisture-advection feedback for the monsoon circulation by lowering the threshold precipitation value. On the other hand the threshold is reached at higher net radiation r_c.

Reserved for Publication Footnotes

Tab. S1: Regional definitions used for data analysis

Monsoon system	INDIA	BAY OF BENGAL	CHINA	W.AFRICA	N.AMERICA	AUSTRALIA
Land region	$70 - 90°E$	$80 - 100°E$	$100 - 110°E$	$15°W - 10°E$	$110 - 100°W$	$120 - 150°E$
	$5 - 30°N$	$15 - 30°N$	$25 - 30°N$	$2 - 14°N$	$20 - 30°N$	$18 - 10°S$
Ocean region	$65 - 78°E$	$80 - 100°E$	$80 - 100°E$	$28°W - 10°E$	$120 - 110°W$	$100 - 130°E$
	$5 - 30°N$	$10 - 20°N$	$10 - 20°N$	$5°S - 14°N$	$20 - 30°N$	$10 - 0°S$
Wind region	$65 - 78°E$	$80 - 100°E$	$90 - 105°E$	$15°W - 10°E$	$111 - 109°W$	$100 - 130°E$
	$5 - 30°N$	$15 - 30°N$	$15 - 25°N$	$2 - 9°N$	$20 - 30°N$	$10°S - 0°$
Monsoon season	JJA	JJA	JJA	JAS	JJA	JFM

Addition of constant equatorial easterlies. The effect of a constant inflow of moist air leads to an addition of a constant w_t to the winds in the heat balance and moisture balance equations

$$lp - w(w + w_t) + r = 0 \qquad \textbf{[S9]}$$
$$(w + w_t)(1 - p) - p = 0 \qquad \textbf{[S10]}$$

yielding the governing equation

$$w^3 + (2w_t + 1)w^2 - (l + r - w_t(w_t + 1))w - ((1 + w_t)r + lw_t) = 0 \qquad \textbf{[S11]}$$

and a shift of the critical threshold towards lower radiation and precipitation values (figure S7).

Addition of stabilizing radiative feedback. Adding a negative contribution $-\sigma'T_L$ to the heat balance may be used to parameterize a stabilizing temperature feedback due to changes in long wave radiation. This addition transforms the non-dimensional heat balance into

$$lp - (w + \sigma)w - \sigma t_O + r = 0 \qquad \textbf{[S12]}$$

where $\sigma \equiv \sigma'/(C_p\beta)$ and $t_O \equiv T_O\alpha\epsilon/\beta$ is the nondimensional atmospheric temperature over the ocean. The resulting governing equation

$$w^3 + (\sigma + 1)w^2 - (l + r - \sigma(\sigma + 1))w - (r + \sigma t_O) = 0 \qquad \textbf{[S13]}$$

resembles the corresponding relation with additional trade winds (figure S8).

Addition of threshold for precipitation. Adding a threshold moisture value q_{th} to equation [4] above which precipitation is initiated does not change the governing equation after redefining $p \equiv P/((q_O - q_{th})\beta)$. It however changes the physical quantities. Critical precipitation then reduces to zero when the threshold value approaches q_O.

1. **Hansen J, *et al*. (1983) Efficient three-dimensional global models for climate studies: Models I and II. *Monthly Weather Review* 111:609–662.**
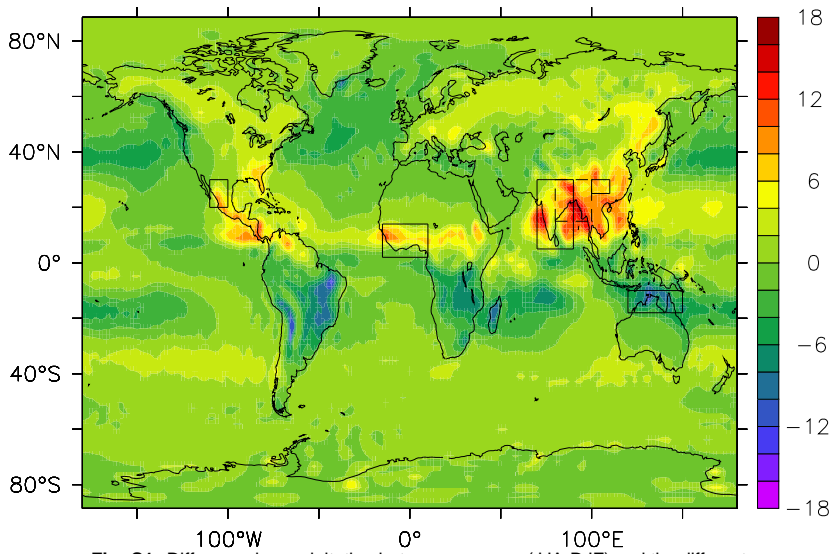
Fig. S1. Difference in precipitation between seasons (JJA-DJF) and the different monsoon regions studied (black boxes).

India

Bay of Bengal

West Africa

North America

China

Australia
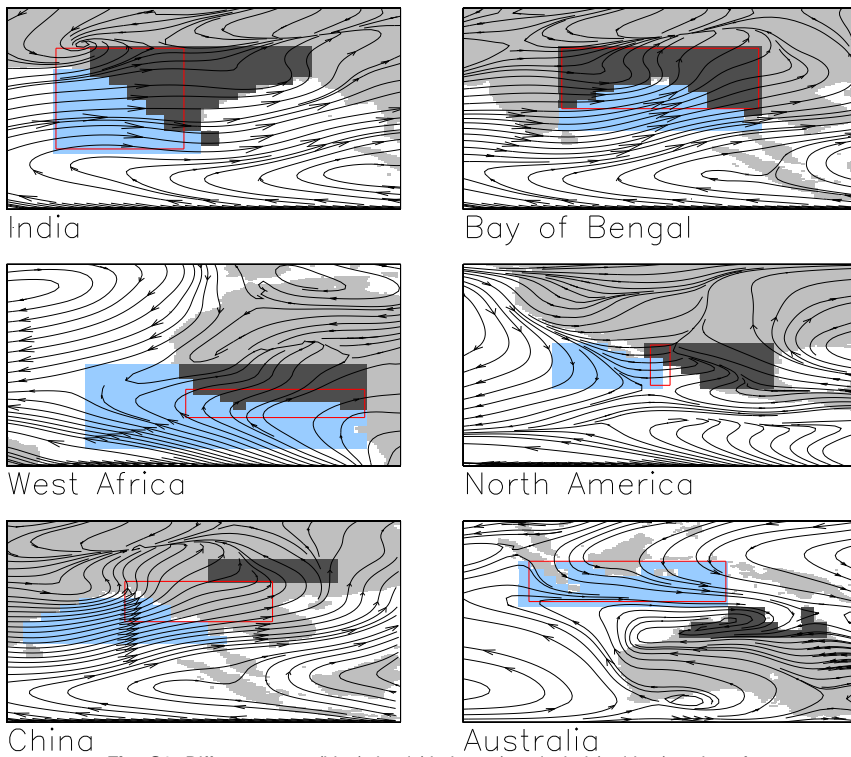
Fig. S2. Different ocean (blue), land (dark gray) and wind (red box) regions for the different monsoon systems as used for computation of the different quantities used to motivate the conceptual model. Flow lines represent summer winds connecting the ocean with the land region.
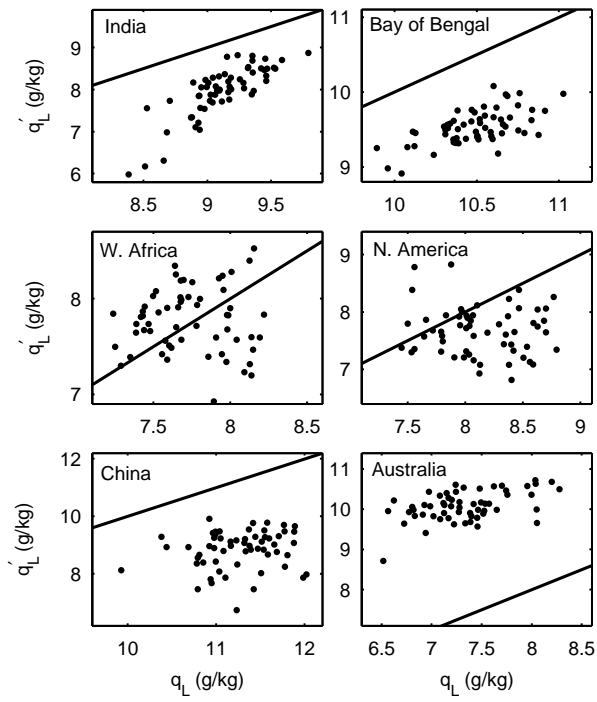
Fig. S3. Specific humidity q'_L over land as computed by the model from time series for precipitation, radiation, temperature difference and specific humidity over the ocean versus observed mean specific humidity over land q_L. The line gives the unit function $q'_L = q_L$
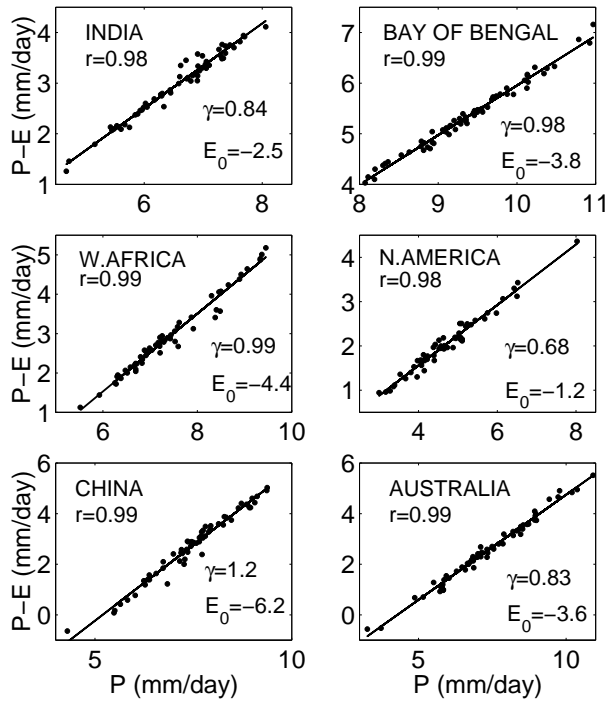
Fig. S4. Scaling of precipitation minus evaporation with precipitation in NCEP-NCAR reanalysis data.
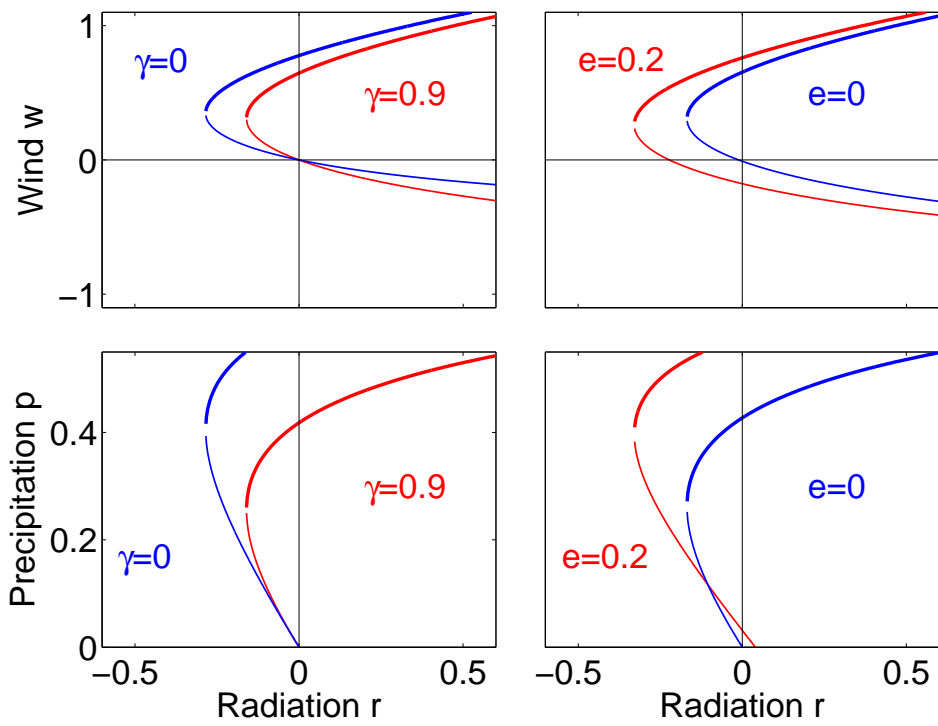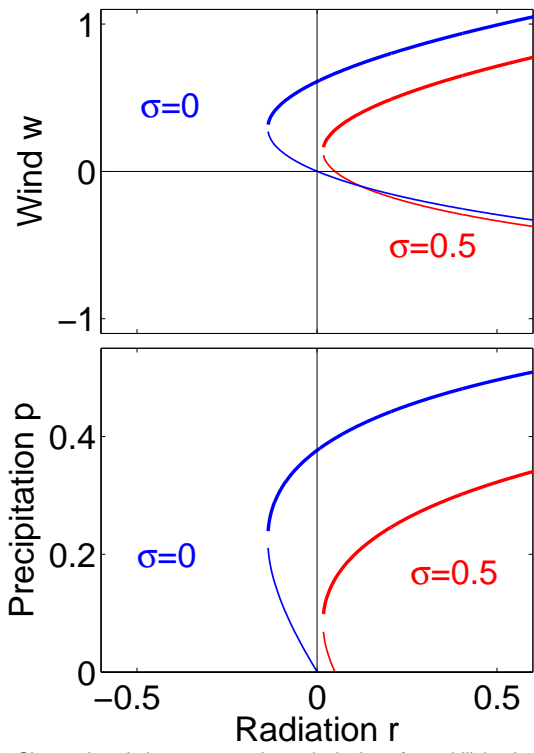
Fig. S5. Change in solution structure due to inclusion of evaporation. Left: constant offset $e = 0.2$ without linear dependence on precipitation $\gamma = 1$ (equation [S4]). Right: linearly dependent evaporation $\gamma = 0.9$ without constant offset $e = 0$.
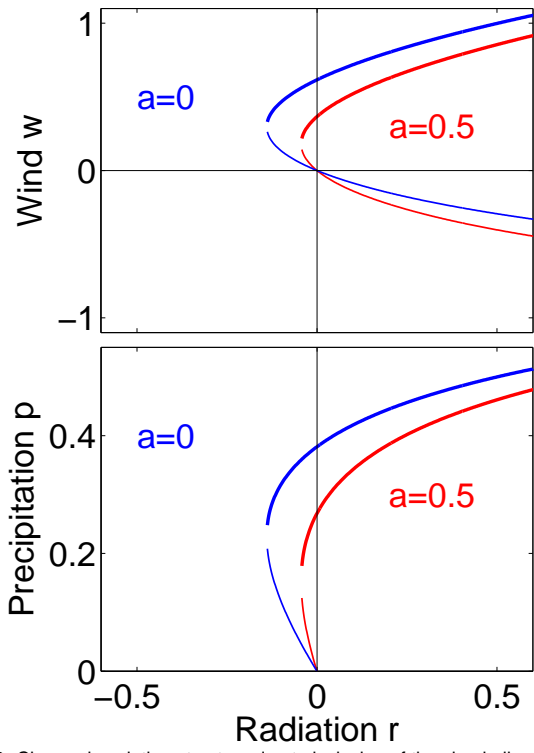
Fig. S6. Change in solution structure due to inclusion of the cloud-albedo feedback
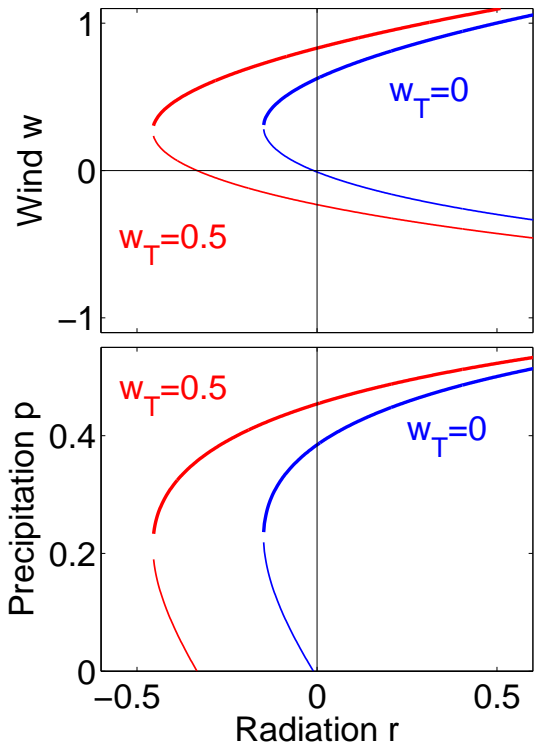
Fig. S7. Change in solution structure due to inclusion of an inflow of moisture and heat by constant trade winds

Fig. S8. Change in solution structure due to inclusion of a stabilizing long wave radiation feedback